nature synthesis

Article

https://doi.org/10.1038/s44160-024-00566-w

Hexafluoroisopropanol-assisted selective intramolecular synthesis of heterocycles by single-electron transfer

Received: 24 October 2023

Accepted: 14 May 2024

Published online: 1 July 2024

Check for updates

Jiale Xie[1,2,3], Jiayu Zhang[1,2,3], Sitthichok Kasemthaveechok[1], Sara López-Resano[1,2], Eric Cots[1], Feliu Maseras[1] ✉ & Mónica H. Pérez-Temprano[1] ✉

Intramolecular amination of remote aliphatic C–H bonds via hydrogen-atom transfer reactions has become a powerful tool for accessing saturated nitrogen-containing heterocycles. However, the formation of six-membered rings or oxa-heterocycles remains a formidable challenge for Hofmann–Löffler–Freytag reactions. Here we show how by simply combining bench-stable (bis(trifluoroacetoxy)iodo)benzene and hexafluoroisopropanol (HFIP) we can switch from the well-established Hofmann–Löffler–Freytag mechanism to a different versatile reaction pathway that enables selective C(sp^3)–H bond functionalization. We have exploited the facile formation of radical cations via single-electron transfer, in the presence or absence of light, to synthesize pyrrolidines and piperidines, including drug-type molecules, along with O-heterocycles. Experimental and computational mechanistic studies support two distinct mechanistic pathways, depending on the electron density of the substrate, in which the HFIP plays a multifunctional role.

Cleavage of C(sp^3)–H bonds via hydrogen-atom transfer (HAT) provides access to reaction pathways that have opened up very exciting possibilities in synthetic organic chemistry[1–3]. One of the pioneering examples of the practical utility of this approach is the classical Hofmann–Löffler–Freytag (HLF) reaction, discovered more than a century ago (Fig. 1)[4–8]. These metal-free protocols enable the transformation of acyclic amines into saturated nitrogen-containing heterocycles (SNHets) through the formation of an amidyl radical that triggers the intramolecular abstraction of δ C–H bonds. Despite important advances in synthetic applicability and the milder nature of the reported reaction conditions due to the exploitation of hypervalent iodine(III) reagents (HIRs)[9–11], such as (bis(trifluoroacetoxy)iodo)benzene (PhI(OTFA)$_2$, PIFA) or (diacetoxyiodo)benzene (PhI(OAc)$_2$, PIDA), persistent challenges associated with these intramolecular C(sp^3)–H aminations remain[2,8,12,13]. The high bond-dissociation free energy of N–H bonds (107–110 kcal mol^{-1}), hampers the homolytic cleavage generating the nitrogen-centred radical[14,15]. Thus, the efficient in situ generation of this open-shell species requires an additional halogenation step for prefunctionalizing the starting material into an N-halogenated amine. Furthermore, the HLF methodology exhibits a high regioselectivity towards five-membered SNHet formation because 1,6-HAT processes are kinetically disfavoured even for benzylic positions[16]. As a result, access to piperidine derivatives, the most frequent nitrogen heterocycle in medicinal chemistry[17,18], is rare and mainly occurs when the formation of pyrrolidines is not viable[19]. Additionally, this reactivity cannot be translated to constructing lactones from carboxylic acids due to undesired Hunsdiecker decarboxylation processes[20–24].

Reports on intramolecular amination[25–27] prompted us to engineer a general and mild strategy that could complement the traditional HLF reactivity and additional nitrogen to carbon radical relays[19,28,29] by the engagement of an HIR in a distinct mechanistic paradigm that circumvents the intramolecular HAT process. Specifically, we envisioned that

[1]Institute of Chemical Research of Catalonia (ICIQ), Tarragona, Spain. [2]Departament de Química Analítica i Química Orgánica, Universitat Rovira i Virgili, Tarragona, Spain. [3]These authors contributed equally: Jiale Xie, Jiayu Zhang. ✉e-mail: fmaseras@iciq.es; mperez@iciq.es

https://doi.org/10.1038/s44160-024-00566-w

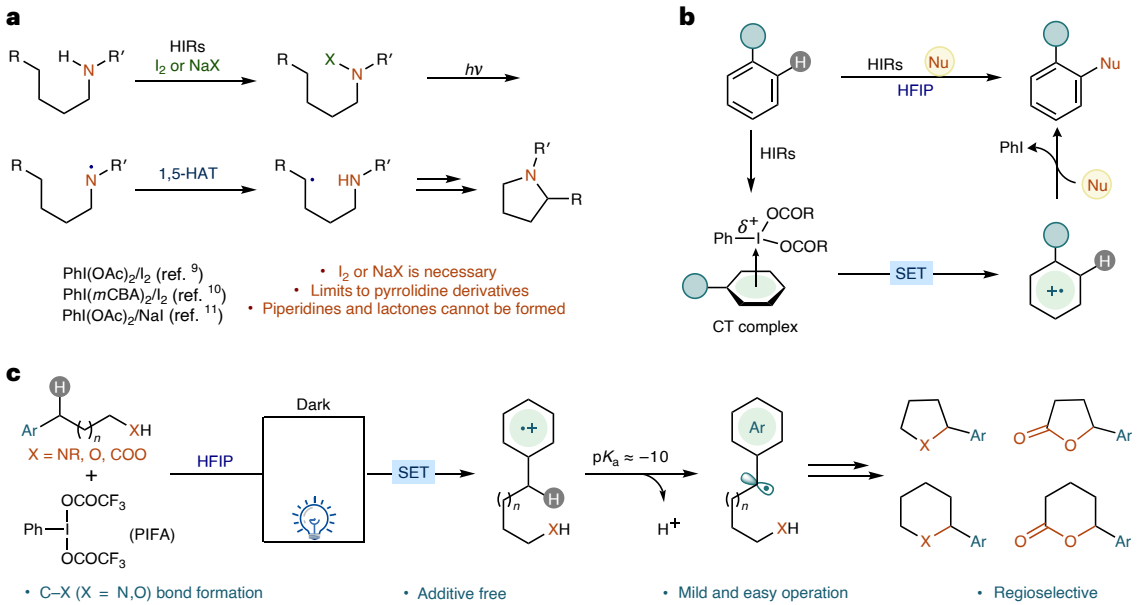

Fig. 1 | Overview of previous studies and this work. a, HLF modification[9–11]. **b**, C(sp^2)–H functionalization through an intracomplex SET process in which a CT complex forms between HIRs and electron-rich aromatic substrates. **c**, HFIP-mediated intramolecular C(sp^3)–H functionalization (this work). *m*CBA, 3-chlorobenzoate.

simply in the absence of the amidyl radical mediator, a single-electron transfer (SET) between the substrate and the HIR could unlock access to radical cation intermediates that switch the mechanism of the C(sp^3)–H cleavage by increasing its acidity[26]. Our inspiration for this strategy lies in seminal studies by Kita and co-workers in which hypervalent derivatives were used to mediate the oxidative nucleophilic C–H functionalization of arenes. The umpolung reactions proceed via radical cations triggered by SET through charge-transfer (CT) complexes of HIRs and electron-rich aromatic substrates[30–35]. These oxidative SET events have been successfully applied to inter- and intramolecular C(sp^2)–H functionalization reactions with a wide array of nucleophiles[36]. Nonetheless, the translation of this mechanistic concept towards electron-deficient scaffolds or the expansion towards the functionalization of C(sp^3)–H bonds remains unexplored.

In this article, we demonstrate that an SET mechanism between HIRs and aromatic substrates grants access to radical cations that initiate the regioselective intramolecular functionalization of C(sp^3)–H bonds. Specifically, we show two radical-cation-generating strategies, depending on the electron density of the substrate. Whereas arenes decorated with electron-donating groups by resonance can undergo SET via CT complexation with PIFA, a photoinduced SET is required when the CT complex is not accessible. We found that 1,1,1,3,3,3-hexafluoro-2-propanol (HFIP), widely recognized by its unique physicochemical properties in C–H functionalization reactions[37–40], is key to promote this established intramolecular reactivity by playing a multifunctional role. It facilitates effective CT-complex formation with electron-rich aromatic substrates[41] and enhances the oxidation ability of PIFA by generating an excited triplet state under blue light-emitting diode (LED) irradiation. This perfluorinated alcohol can also stabilize the radical cation intermediates resulting after the SET oxidation[42,43], and can cause a second SET event leading to a carbocation that is intercepted intramolecularly by the attack of the tethered nucleophile. This mild and simple hypervalent iodine(III)-mediated strategy gives selective access to a broad scope of valuable five- and six-membered saturated heterocycles, including biorelevant compounds, which are difficult to synthesize under HLF conditions. This discovery broadens the synthetic utility of HIRs in metal-free C(sp^3)–H functionalization reactions and intramolecular cyclizations. Experimental, spectroscopic and computational studies support the proposed mechanistically divergent SET-based pathway.

Results and discussion

We started our study by evaluating the feasibility of an SET between PIFA and **1a** through CT complexation. We envisioned that the electron-rich aromatic fragment of the amine could serve as a donor and interact with the HIR in HFIP, generating a radical cation[30,34,44–46]. Whereas the separate solutions of **1a** and PIFA in HFIP were colourless, their mixture immediately turned a pale yellow, suggesting the formation of a CT complex. Ultraviolet–visible and electron paramagnetic resonance (EPR) studies provide further support for the SET event (Fig. 2a). The absorption spectrum of this mixture exhibited an intense absorption band in the visible region between 400 and 500 nm, which indicated the formation of the radical cation, **Int-I**[30,47,48], which was also detected by electron paramagnetic resonance spectroscopy (Fig. 2b)[47,49]. After proving the ability of the PIFA–**1a** system to participate in SET events, we aimed to translate this finding into the development of an intramolecular C(sp^3)–H amination reaction. We found that the reaction of **1a** with 1.2 equiv. of PIFA in HFIP at room temperature provided the desired nitrogen-based heterocycle **2a** in a 62% isolated yield. Control experiments showed that the reactivity was completely inhibited when using PIDA or other solvents, indicating that the PIFA/HFIP combination is key for the successful implementation of a synthetic SET strategy through radical cation generation (Fig. 2c).

Adopting the reaction conditions described in Fig. 2c, we next determined the generality of our protocol (Fig. 2d). Substrates containing different electron-donating groups, such as pyrrolidine or aromatic fragments, provided the desired products (**2b**–**2d**) in moderate to excellent yields, including **2c** in gramme scale. As anticipated, the same strategy successfully facilitated the formation of piperidine within a six-membered cyclization (**2e**–**2f**), which cannot be easily achieved through the HLF methodology due to the kinetically disfavoured 1,6-HAT process. For comparison, using PIDA instead of PIFA, and conditions suitable for the HLF process, was less efficient at producing **2f** and formed considerable amounts of five-membered ring by-products. Furthermore, this methodology extends beyond C–H amination, allowing oxygen nucleophiles to capture the benzylic cation and obtain the lactone product **2g** and ether product **2h** with yields of 77% and 60%, respectively. By contrast, the absence of donating groups with resonance effect on the aromatic architecture greatly affects the efficiency of the process. Substrates adorned with 4-(*tert*-butyl)

https://doi.org/10.1038/s44160-024-00566-w

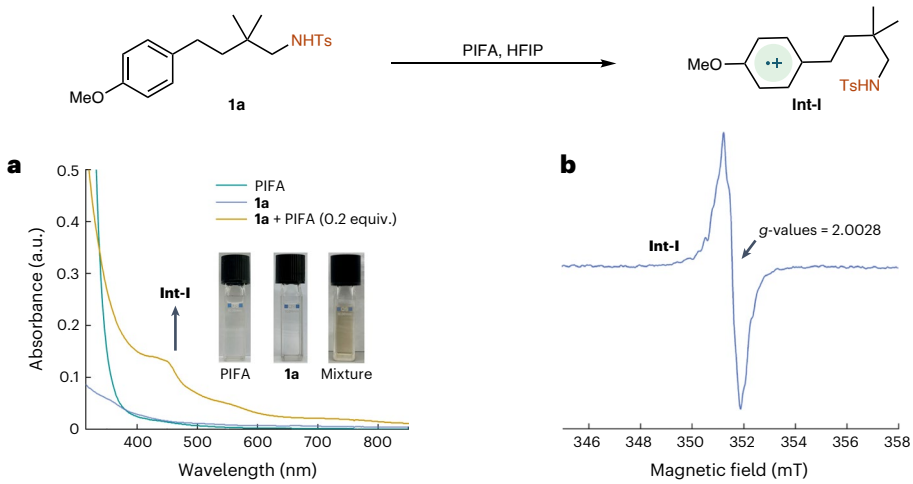

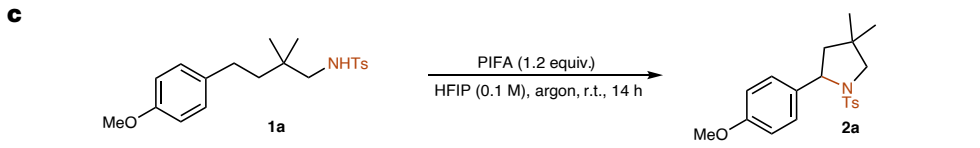

Entry	Variation from standard condition	**2a** (% yield)
1	None	72 (62)[a]
2	PIDA instead of PIFA	NR
3	DCM instead of HFIP	NR
4	2-Propanol instead of HFIP	NR
5	MeCN instead of HFIP	15
6	$PhCF_3$ instead of HFIP	Trace

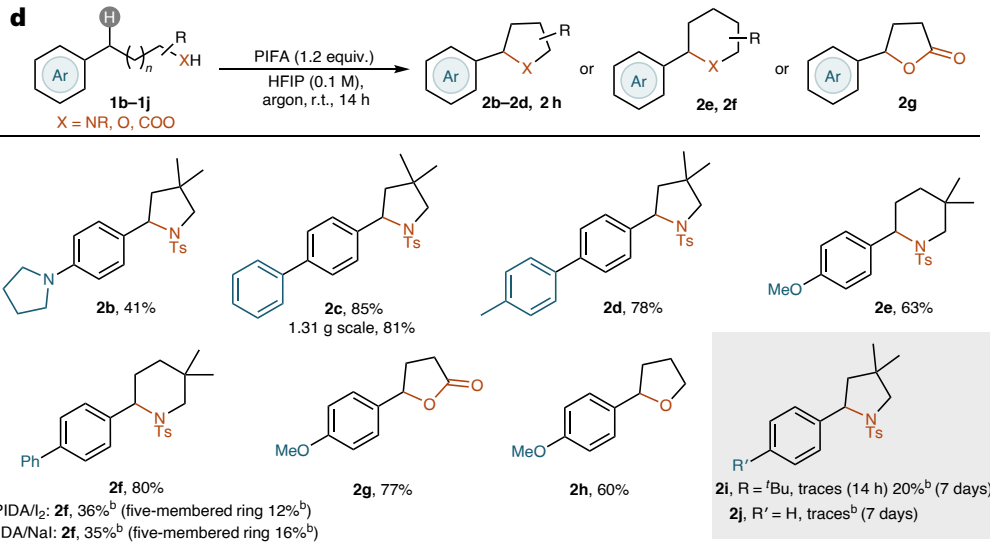

Fig. 2 | HFIP-assisted intramolecular C(sp^3)–H functionalization through an intracomplex SET process with a CT complex. a, Ultraviolet–visible spectra of **1a**, PIFA, and a mixture of **1a** and PIFA in HFIP and images of the corresponding solutions. **b**, EPR measurement of the reaction mixture of **1a** and PIFA (1.2 equiv.) in HFIP. **c**, Control experiments. Reaction conditions: **1a** (0.05 mmol, 1.0 equiv.), HIR (0.06 mmol, 1.2 equiv.) in solvent (0.5 ml), at room temperature under argon for 14 h. Yields were determined by crude ^{1}H NMR spectroscopy analysis using 1,1,2,2-tetrachloroethane as the internal standard. [a]Isolated yield. **d**, Scope of the intramolecular C(sp^3)–H functionalization. Reaction conditions: **1** (0.15 mmol, 1.0 equiv.), PIFA (0.18 mmol, 1.2 equiv.) in HFIP (0.1 M) at room temperature under argon for 14 h. Isolated yields. [b]Yields were determined by crude ^{1}H NMR spectroscopy analysis using 1,1,2,2-tetrachloroethane as the internal standard. Ts, toluenesulfonyl; DCM, dichloromethane; NR, no reaction.

phenyl or phenyl moieties only afforded traces of **2i** and **2j** under these conditions.

In an attempt to overcome the difficulties caused by using starting materials containing non-electron-rich arenes, we sought to interrogate the structure–activity relationship for substitution of the aryl scaffold. We noticed a difference in the reaction mixture when using **1j** as starting material rather than **1a**. Instead of a pale-yellow solution, there was no change in colour when this compound was mixed with PIFA in HFIP. This was also confirmed by ultraviolet–visible spectroscopy: the mixture provided the same absorption spectrum as PIFA alone, indicating that this starting material is not capable of interacting with the HIR (Fig. 3a). Furthermore, an electrochemical analysis showed a clear correlation between the electron-donating ability of the functional groups on the aromatics and the oxidation potential of the

https://doi.org/10.1038/s44160-024-00566-w

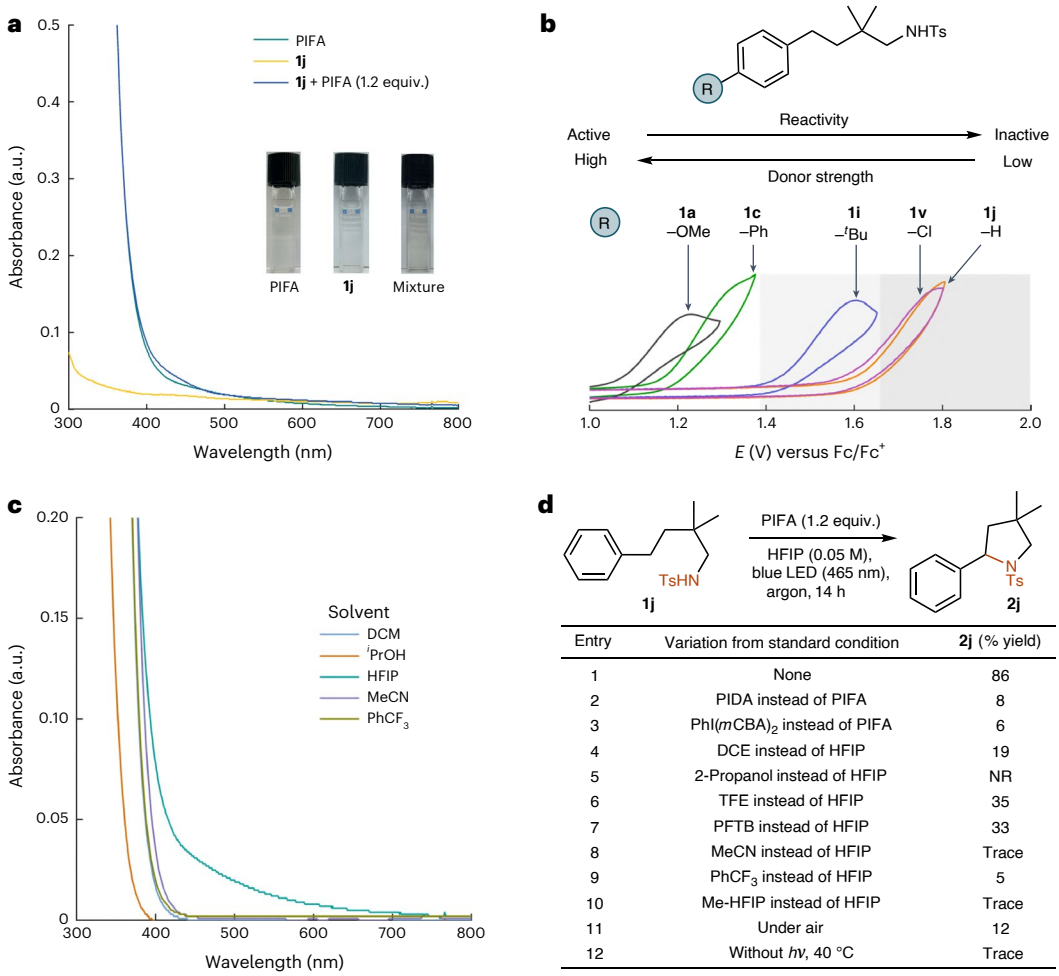

Entry	Variation from standard condition	**2j** (% yield)
1	None	86
2	PIDA instead of PIFA	8
3	PhI(*m*CBA)$_2$ instead of PIFA	6
4	DCE instead of HFIP	19
5	2-Propanol instead of HFIP	NR
6	TFE instead of HFIP	35
7	PFTB instead of HFIP	33
8	MeCN instead of HFIP	Trace
9	$PhCF_3$ instead of HFIP	5
10	Me-HFIP instead of HFIP	Trace
11	Under air	12
12	Without *hν*, 40 °C	Trace

Fig. 3 | C(sp^3)–H functionalization of non-electron-rich arenes. a, Ultraviolet–visible absorption spectra of **1j**, PIFA, and a mixture of **1j** and PIFA (1.2 equiv.) and images of the corresponding solutions. **b**, Systematic evaluation of the electron-donating group effect in C(sp^3)–H functionalization by cyclic voltammetry in HFIP using Fc/Fc$^+$ as a reference. **c**, Ultraviolet–visible absorption spectra of PIFA in different solvents. **d**, Screening of photoredox C(sp^3)–H amination. Reaction conditions: **1j** (0.05 mmol, 1.0 equiv.), PIFA (0.06 mmol, 1.2 equiv.) in HFIP (0.05 M) under illumination by a blue LED strip (λ_{max} = 465 nm, 14 W) at room temperature for 14 h. Yields were determined by crude ^{1}H NMR spectroscopy analysis using mesitylene as the internal standard; TFE, 2,2,2-trifluoroethanol; PFTB, 1,1,1,3,3,3-hexafluoro-2-(trifluoromethyl)-2-propanol; *E*, potential; DCE, dichloroethane.

corresponding substrates in HFIP (Fig. 3b). As expected, **1a** exhibits the strongest donating ability, with an irreversible oxidation potential at 1.23 V versus Fc/Fc$^+$ (Fc, ferrocene). The replacement of the methoxy group by a phenyl substituent (**1c**) provokes an anodic shift of 100 mV, which remains sufficient to promote the CT complexation, as observed experimentally. The decrease in donating strength observed for **1i**, which contains a *tert*-butyl group (**1i**), is in alignment with the poor reactivity observed with our optimal C–N bond-forming reaction condition, requiring at least 7 days to achieve 20% yield of the corresponding five-membered ring. This experimental outcome might indicate that the reaction kinetics was diminished by the lower electron density on the phenyl ring. Finally, substrates without an electron-donating group or with electron-withdrawing functionalities on the aromatic core showed higher oxidation potentials at ~1.75 V versus Fc/Fc$^+$. Therefore, formation of a CT complex between a weak-electron-density substrate and PIFA is not efficient, explaining their inactivity in the intracomplex SET approach.

Interestingly, our ultraviolet–visible study also revealed that PIFA presented absorption bands at wavelengths longer than 450 nm in HFIP, a region inaccessible in alternative solvents (Fig. 3c), which might correspond to spin-forbidden transitions[50,51] Encouraged by this result, we questioned whether the photoexcitation of PIFA could unlock SET mechanisms for non-electron-rich substrates. When we tested the intramolecular C(sp^3)–H amination of **1j** under light irradiation, the desired product was achieved in 86% yield (Fig. 3d, entry 1). Moreover, the replacement of PIFA by PIDA or PhI(*m*CPBA)$_2$ (Fig. 3d, entries 2 and 3) or HFIP by alternative solvents (Fig. 3d, entries 4–10) resulted in a dramatic decrease in reactivity under the same conditions. This highlights the unique match between PIFA and HFIP in the C(sp^3)–H functionalization reaction. The absence of light or the presence of oxygen also reduced the efficiency of the photoinduced SET process (Fig. 3d, entries 11 and 12).

Having established a set of optimized reaction conditions, the scope of this light-assisted intramolecular C(sp^3)–H functionalization protocol was evaluated (Fig. 4a). Pleasingly, the reaction exhibited a wide range of applicability, accommodating various sulfonyl protecting groups on the nitrogen atom. Notably, tosyl, mesyl, 4-bromophenyl sulfonyl, nosyl and triflate groups were well tolerated, providing the corresponding pyrrolidine products in excellent yields (**2i**–**2n**). Additionally, benzamide and trifluoroacetamide derivatives also underwent successful transformations, affording pyrrolidines **2o** and **2p** with good yields. The light-assisted strategy exhibited its advantages by enabling the reactions of substrate with electron-donating as well as electron-withdrawing substituents on the aryl group at the *ortho*, *meta* and *para* positions with excellent yields (**2i**, **2q**–**2w**), which included aryl chloride and bromide functionalities that can be further engaged in

https://doi.org/10.1038/s44160-024-00566-w

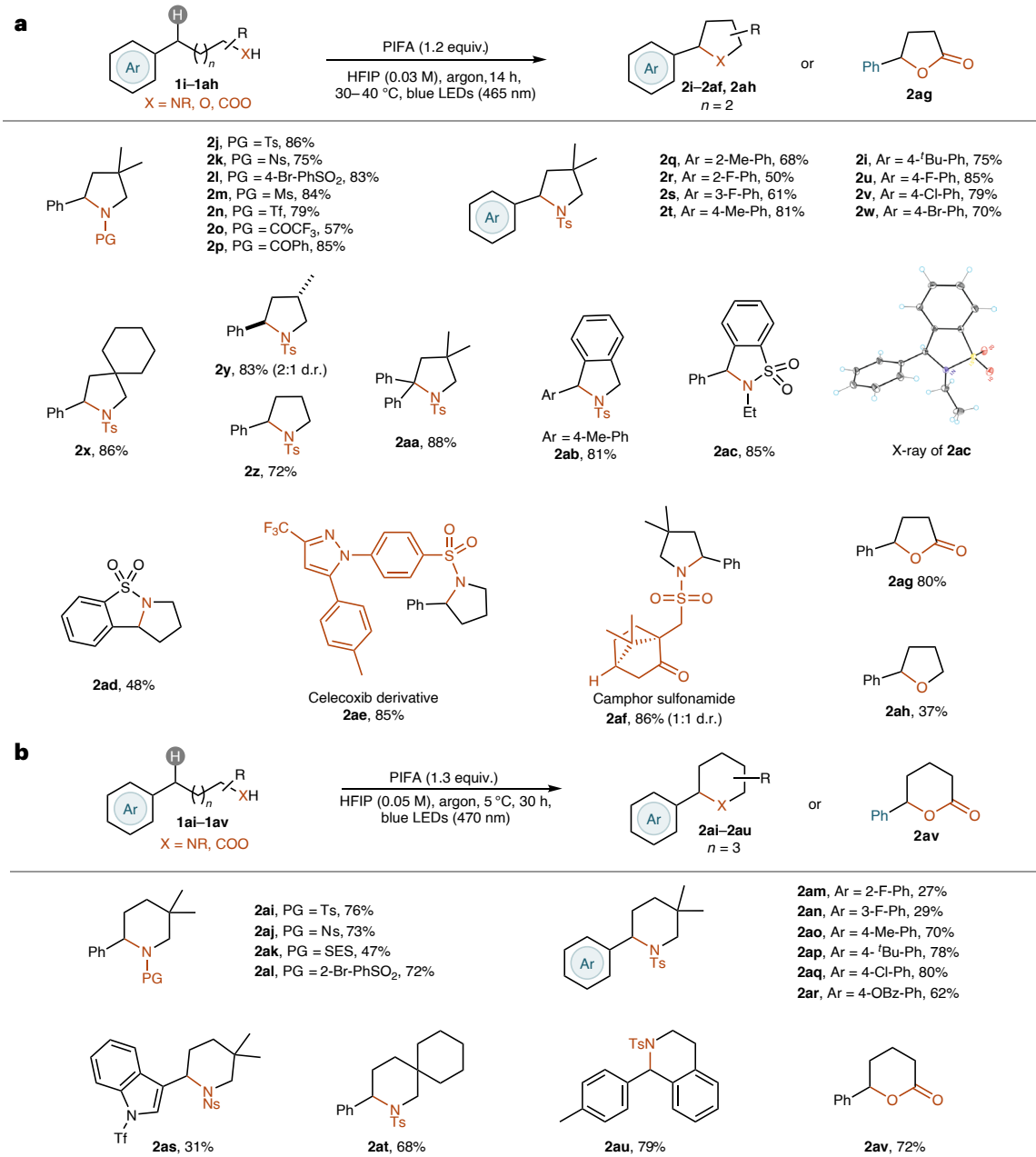

Fig. 4 | Scope of the photoredox C(sp^3)–H functionalization. a, Scope of the intramolecular C(sp^3)–H functionalization for accessing five-membered products. Reaction conditions: **1** (0.15 mmol, 1.0 equiv.), PIFA (0.18 mmol, 1.2 equiv.) in HFIP (0.03 M) at room temperature under illumination by a blue LED strip (λ_{max} = 465 nm, 14 W) for 14 h. Isolated yields. **b**, Scope of the intramolecular C(sp^3)–H functionalization for accessing six-membered products. Reaction conditions: **1** (0.15 mmol, 1.0 equiv.), PIFA (0.195 mmol, 1.3 equiv.) in HFIP (0.05 M) at 5 °C under illumination by a 900 mA blue LED (λ_{max} = 470 nm) for 30 h. Isolated yields. PG, protecting group; Ns, 4-nitrobenzenesulfonyl; Ms, methanesulfonyl; Tf, trifluoromethanesulfonyl; SES, 2-(trimethylsilyl) ethanesulfonyl; Bz, benzyl.

additional modular diversifications. Moreover, we discovered that the transformation can be carried out with modified backbones (**2x**–**2ad**). Particularly noteworthy was the observation of acyclic stereocontrol when used a substrate with monosubstitution in the alkyl chain, leading to a diastereomeric excess of up to 2.1:1 for the *trans*:*cis* ratio (**2y**)[26]. This transformation also works well without geminal alkyl groups, demonstrating its tolerance for substrates without a Thorpe–Ingold effect (**2z**). Additionally, the versatility of the reaction extended to the amination of tertiary benzylic positions, yielding the desired product **2aa** in 88% yield.

To access more intricate molecular frameworks, we incorporated a phenyl backbone into the substrates, leading to the formation of highly desirable isoindoline **2ab** and dioxoisothiazole derivative **2ac** with exceptional yields[52,53], with the latter being unambiguously characterized by X-ray crystallography. Moreover, the reaction demonstrated its potential in synthesizing tricyclic alkaloid products, exemplified by the efficient formation of **2ad** through transannular C–H amination. To showcase its applicability in late-stage amination of complex pharmaceutical and natural products, we explored its use with celecoxib and camphor derivatives, resulting in the formation of products **2ae** and **2af** in excellent yields. In addition to the amination reactions, our methodology also proved effective in lactonization and etherification processes, delivering the corresponding desired products in moderate to high yields (**2ag**–**2ah**). This photochemical strategy also enables

https://doi.org/10.1038/s44160-024-00566-w

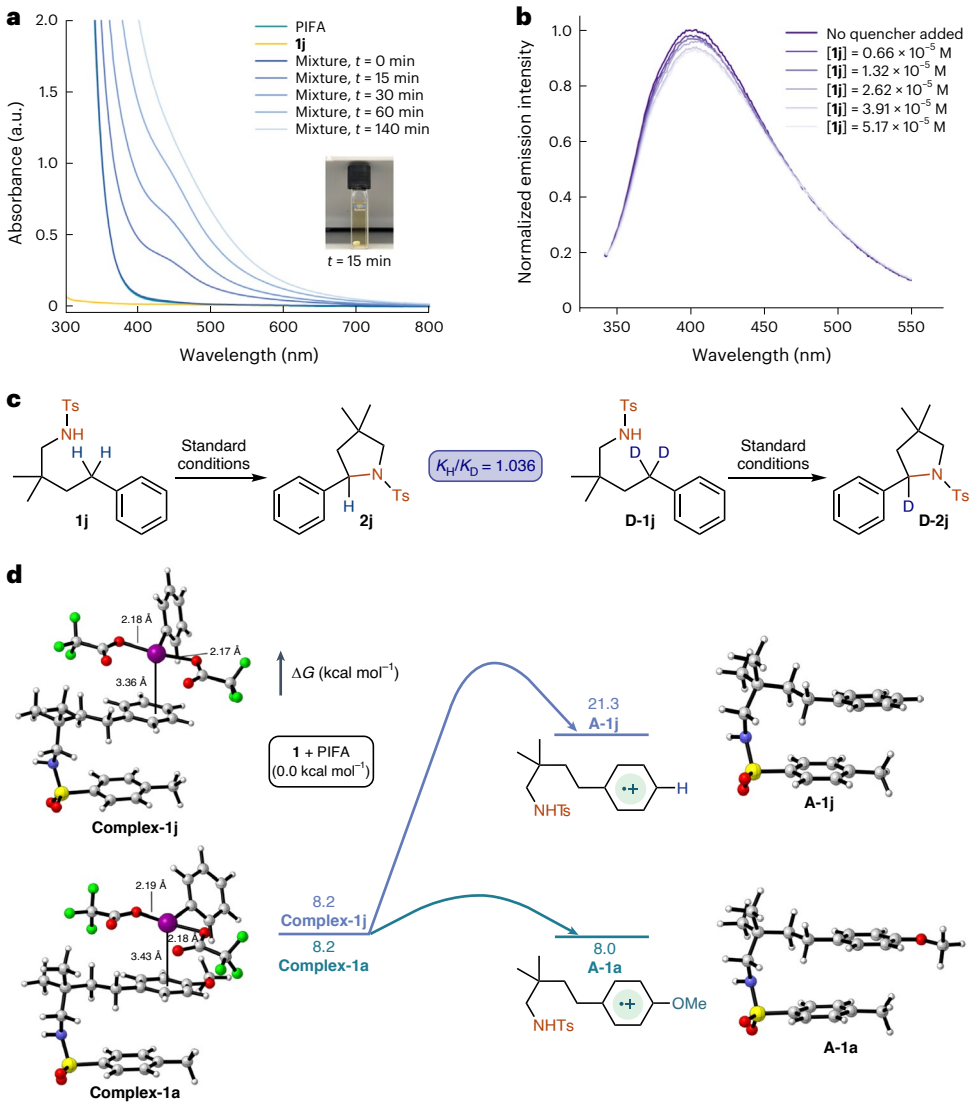

Fig. 5 | Investigation of the mechanism of the photoredox C(sp^3)–H functionalization. a, Ultraviolet–visible absorption spectra of the mixture of **1j** (1.0 equiv.) and PIFA (1.2 equiv.) in HFIP upon irradiation with a blue LED strip (λ_{max} = 465 nm, 14 W) and image of the corresponding mixture after irradiation for 15 min. **b**, Fluorescence quenching studies of excited PIFA by **1j** in HFIP. **c**, Kinetic isotope effect experiments. **d**, Simplified free-energy profile of the CT complex and aromatic radical cation species of **1a** and **1j**. Atom colour coding: blue, nitrogen; green, fluorine; grey, carbon; purple, iodine; red, oxygen; white, hydrogen; yellow, sulfur.

the efficient synthesis of six-membered heterocycles (Fig. 4b). The cyclization process was successful for substrates containing various nitrogen-protecting groups (**2ai**–**2al**). As expected, our methodology exhibited excellent tolerance towards the inclusion of common functional groups at the 2-, 3- and 4-positions of the arene group (**2am**–**2as**), including a heteroaromatic derivative **2as**, showcasing the wide applicability of this transformation. Modifying the backbone of the substrate was also amenable, resulting in the formation of product **2at** with a yield of 68%. Additionally, the reaction proceeded smoothly with a diphenylmethyl derivative, yielding the appealing tetrahydroisoquinoline core with a high yield (**2au**). Moreover, utilizing this process, we were able to obtain the desired lactone product **2av** with a remarkable yield. Furthermore, we demonstrated the facile removal of the nosyl protecting group, providing the free pyrrolidine **3** in excellent yield. This removal step opens avenues for introducing other functionalities on the nitrogen atoms, thus enhancing the potential of our method in medicinal chemistry applications (Supplementary Section 7).

To better understand the reaction mechanism of the photochemical approach, we conducted various experimental and computational studies. Upon irradiation of the mixture of **1j** and PIFA in HFIP with blue LEDs for 15 min, the ultraviolet–visible spectra showed an absorption band in the range of 400–500 nm (Fig. 5a), consistent with the ultraviolet–visible spectra of **1a** obtained in Fig. 2b, indicating the formation of aromatic radical cationic intermediates. A fluorescence quenching study confirmed that the excited PIFA can be quenched by substrate **1j** to provide the corresponding phenyl radical cation (Fig. 5b).

Additionally, a kinetic isotope effect value of 1 was determined through a competition experiment involving **1j** and its deuterated benzylic derivative, **D-1j** (Fig. 5c). This finding aligns perfectly with the initial oxidation process of the aromatic ring. Density functional theory (DFT) calculations at the M06-D3/def2-TZVP/SMD//M06-D3/6-31 G(d)-LANL2DZ/SMD level in HFIP solvent (full computational details are given in the Supplementary Information; computational data have been uploaded to the ioChem-BD repository[54]) confirmed the occurrence of an intracomplex SET process between **1a** and PIFA via a CT complex, with a low-energy intermediate of 8.0 kcal mol^{-1} (Fig. 5d). However, when the same process was investigated between **1j** and PIFA, the corresponding intermediate has an energy as high as 21.3 kcal mol^{-1}.

https://doi.org/10.1038/s44160-024-00566-w

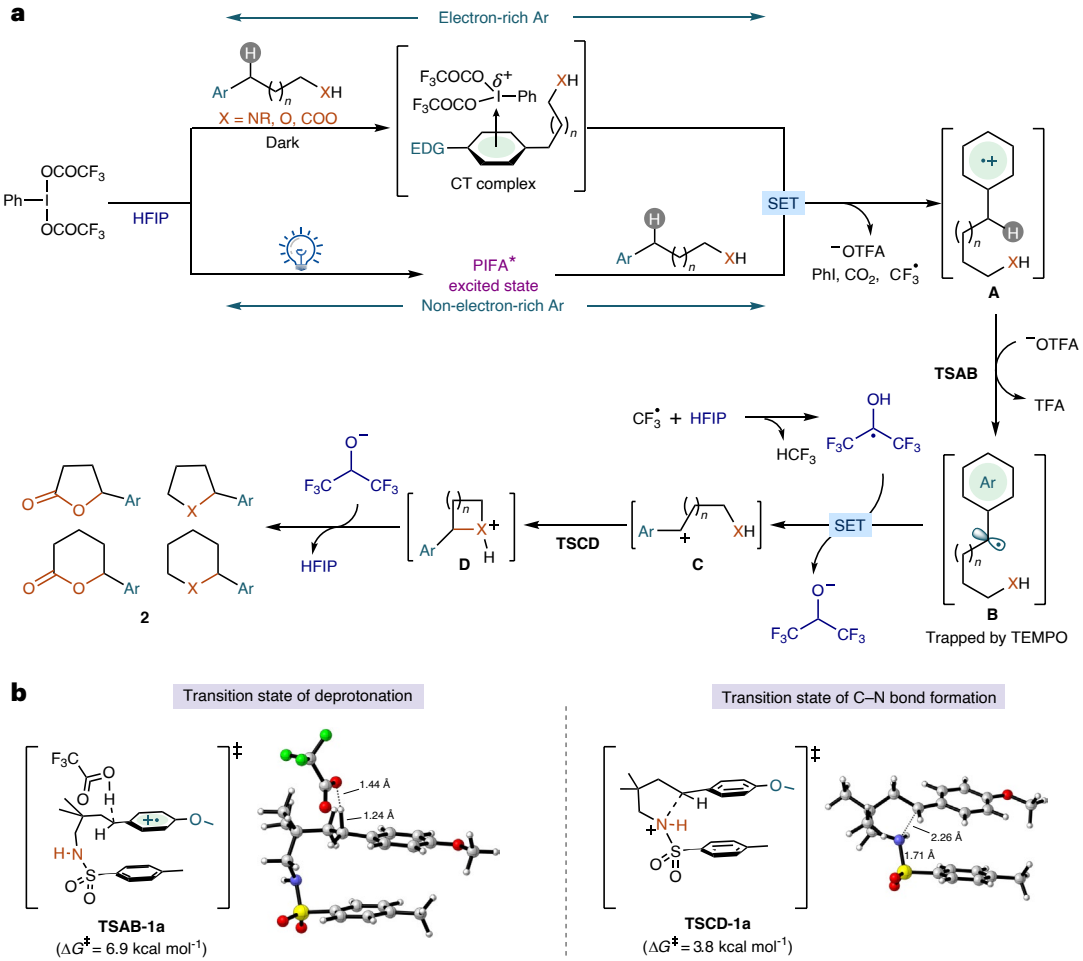

Fig. 6 | Proposed mechanism and transition states. a, Proposed mechanism of selective intramolecular synthesis of heterocycles enabled by SET. **b**, Key computed transition states for deprotonation and C–N bond formation. Atom colour coding: blue, nitrogen; green, fluorine; grey, carbon; red, oxygen; white, hydrogen; yellow, sulfur. EDG, electron-donating group; **TSAB**, transition state **AB**; **TSCD**, transition state **CD**.

This relatively high energy for the intermediate ought to be coupled with a higher barrier, making it impossible for the intracomplex SET process between **1j** and the hypervalent iodine in the ground state to occur. Hence, the use of visible light is necessary to enhance the oxidation ability of PIFA.

Based on the combined experimental and DFT observations, a proposed mechanism is depicted in Fig. 6. The reaction commences with the substrate undergoing an SET process with PIFA, resulting in the formation of the aromatic radical cation **A**. With an electron-rich substrate, **A** is formed through an intracomplex SET of the CT complex in the ground state. On the other hand, visible-light excitation turns PIFA into a strong oxidizing agent (E_{red} (PIFA*/PIFA^{-}) = 3.09 V versus Fc/Fc^{+}) in HFIP, as estimated from spectroscopic measurements and the oxidation potential of PIFA reported in the literature (Supplementary Section 9.6)[41]. The lower oxidation potential of substrate **1j** (E_{ox} (**1j**/**1j**$^{\cdot+}$) = 1.78 V versus Fc/Fc^{+} in HFIP, Fig. 3b) indicates that it is particularly effective at enabling the SET event, leading to the formation of intermediate **A**. At this stage, the acidity of the benzylic proton experiences a notable increase, rendering it an exceptionally strong acid that can be readily deprotonated[23,55–57]. This deprotonation leads to the formation of the benzylic radical **B**, with the assistance of the in situ generated trifluoroacetate anion, which is detected by using (2,2,6,6-tetramethylpiperidin-1-yl)oxyl (TEMPO) as a radical trap (Supplementary Section 9.8). Subsequently, **B** undergoes a further single-electron oxidation by the HFIP radical, which is formed through a favourable HAT process involving the CF_3 radical and HFIP. The generation of the CF_3 radical was confirmed by the detection of CO_2 using gas chromatography after the reaction in both dark and photoredox processes. The oxidation of **B** leads to the formation of the benzylic cation **C**, which is then captured by the nucleophilic fragment, resulting in the corresponding heterocyclic product. Additionally, we conducted DFT calculations on the mechanism. The results reveal activation energies of 6.9 kcal mol^{-1} for deprotonation (**TSAB-1a**) and 3.8 kcal mol^{-1} for the formation of the C–N bond (**TSCD-1a**) (Fig. 6b). For comparison, the intramolecular radical addition of intermediate **B** has also been investigated[58]. However, this process via a transition state **TSBE-1a** ($\Delta G^{‡}$ = 38.1 kcal mol^{-1}) requires a higher activation free energy than the proposed mechanism. Removal of one electron from intermediate **B-1a** to lead to intermediate **C-1a** is much more favoured (Supplementary Fig. 18).

Conclusion

We have developed a PIFA-mediated intramolecular C(sp^3)–H functionalization reaction facilitated by HFIP to access valuable pyrrolidines, piperidines and O-heterocycles. The success of this reaction relies on the SET process, leading to the formation of an aromatic radical cation intermediate. The reaction proceeds through two distinct pathways, depending on the electron density of the substrate's arene ring, which were confirmed by both experimental and theoretical mechanistic studies. For electron-rich substrates, the SET process takes place via a CT complex formed between PIFA and the substrate. However, for substrates without electron-donating substituents, the process occurs

with the assistance of blue light. Under these reaction conditions, HFIP plays a key multifunctional role: from facilitating CT complex formation and enhancing the oxidation ability of PIFA to enabling the stabilization of the radical cation intermediate. This protocol features mild reaction conditions and excellent regioselectivity, achieving C(sp^3)–H functionalization via an SET process of the CT complex formed between the electron-rich substrate with HIRs. Furthermore, it opens a synthetic avenue for the functionalization of substrates that cannot form CT complexes with HIRs.

Methods

General protocol for C(sp^3)–H functionalization without light irradiation

The sulfonamide (0.15 mmol, 1.0 equiv.) and PIFA (1.2 equiv.) were added to a reaction vial equipped with a stir bar. This reaction vial was then placed in an argon-filled glovebox, 1.5 ml of dry HFIP was added to the mixture and the reaction vial was sealed with a cap equipped with a Teflon septa. The sealed vial was removed from the glovebox and stirred at room temperature for 14 h. After completion of the reaction, volatiles were evaporated under reduced pressure and the resulting crude product was purified by chromatography to obtain the final product.

General protocol for C(sp^3)–H functionalization for five-membered rings with light irradiation

Reactions were performed using set-up 1 in Supplementary Fig. 1. The sulfonamide (0.15 mmol, 1.0 equiv.) and PIFA (1.2 equiv.) were added to a reaction vial equipped with a stir bar. This reaction vial was then placed in an argon-filled glovebox, 4.5 ml of dry HFIP was added to the mixture and the reaction vial was sealed with a cap equipped with a Teflon septa. The vial was then carefully removed from the glovebox and subjected to irradiation under stirring for 14 h. After completion of the reaction, volatiles were evaporated under reduced pressure and the resulting crude product was purified by chromatography to obtain the final product.

General protocol for C(sp^3)–H functionalization for six-membered rings with light irradiation

Reactions were performed using set-up 2 in Supplementary Fig. 2. The sulfonamide (0.15 mmol, 1.0 equiv.) and PIFA (1.3 equiv.) were added to a reaction vial equipped with a stir bar, this reaction vial was then placed in an argon-filled glovebox, 3.0 ml of dry HFIP was added to the mixture and the reaction vial was sealed with a cap equipped with a Teflon septa. The vial was then carefully removed from the glovebox and subjected to irradiation under stirring at 5 °C for 30 h. After completion of the reaction, volatiles were evaporated under reduced pressure and the resulting crude product was purified by chromatography to obtain the final product.

Data availability

All data are available in the main text or the Supplementary Information. CCDC 2282188 contain the supplementary crystallographic data for this paper. This data can be obtained free of charge via www.ccdc.cam.ac.uk/data_request/cif. This study did not generate any code. A dataset collection of computational results is available as source data with this paper and can be accessed at ioChem-BD repository via https://doi.org/10.19061/iochem-bd-1-327. Source data are provided with this paper.

References

1. Mayer, J. M. Understanding hydrogen atom transfer: from bond strengths to Marcus theory. *Acc. Chem. Res.* **44**, 36–46 (2011).
2. Stateman, L. M., Nakafuku, K. M. & Nagib, D. A. Remote C–H functionalization via selective hydrogen atom transfer. *Synthesis* **50**, 1569–1586 (2018).
3. Capaldo, L., Ravelli, D. & Fagnoni, M. Direct photocatalyzed hydrogen atom transfer (HAT) for aliphatic C–H bonds elaboration. *Chem. Rev.* **122**, 1875–1924 (2022).
4. Hofmann, A. W. Ueber die einwirkung des broms in alkalischer Lösung auf die amine. *Ber. Dtsch. Chem. Ges.* **16**, 558–560 (1883).
5. Löffler, K. & Freytag, C. Über eine neue bildungsweise von N-alkylierten pyrrolidinen. *Ber. Dtsch. Chem. Ges.* **42**, 3427–3431 (1909).
6. Jeffrey, J. L. & Sarpong, R. Intramolecular C(sp^3)–H amination. *Chem. Sci.* **4**, 4092–4106 (2013).
7. Xiong, T. & Zhang, Q. New amination strategies based on nitrogen-centered radical chemistry. *Chem. Soc. Rev.* **45**, 3069–3087 (2016).
8. Zhang, J. & Pérez-Temprano, M. H. Intramolecular C(sp^3)–H bond amination strategies for the synthesis of saturated N-containing heterocycles. *Chimia* **74**, 895–903 (2020).
9. de Armas, P. et al. Synthesis of 1,4-epimine compounds. Iodosobenzene diacetate, an efficient reagent for neutral nitrogen radical generation. *Tetrahedron Lett.* **26**, 2493–2496 (1985).
10. Martínez, C. & Muñiz, K. An iodine-catalyzed Hofmann–Löffler reaction. *Angew. Chem. Int. Ed.* **54**, 8287–8291 (2015).
11. Wappes, E. A., Fosu, S. C., Chopko, T. C. & Nagib, D. A. Triiodide-mediated δ-amination of secondary C–H bonds. *Angew. Chem. Int. Ed.* **55**, 9974–9978 (2016).
12. Reddy Kandimalla, S., Prathima Parvathaneni, S., Sabitha, G. & Subba Reddy, B. V. Recent advances in intramolecular metal-free oxidative C–H bond aminations using hypervalent iodine(III) reagents. *Eur. J. Org. Chem.* **2019**, 1687–1714 (2019).
13. Guo, W., Wang, Q. & Zhu, J. Visible light photoredox-catalysed remote C–H functionalisation enabled by 1,5-hydrogen atom transfer (1,5-HAT). *Chem. Soc. Rev.* **50**, 7359–7377 (2021).
14. Bordwell, F. G. & Ji, G. Z. Effects of structural changes on acidities and homolytic bond dissociation energies of the H–N bonds in amidines, carboxamides, and thiocarboxamides. *J. Am. Chem. Soc.* **113**, 8398–8401 (1991).
15. Bordwell, F. G., Zhang, S., Zhang, X. M. & Liu, W. Z. Homolytic bond dissociation enthalpies of the acidic H–A bonds caused by proximate substituents in sets of methyl ketones, carboxylic esters, and carboxamides related to changes in ground state energies. *J. Am. Chem. Soc.* **117**, 7092–7096 (1995).
16. Nechab, M., Mondal, S. & Bertrand, M. P. 1,*n*-Hydrogen-atom transfer (HAT) reactions in which $n \neq 5$: an updated inventory. *Chem. Eur. J.* **20**, 16034–16059 (2014).
17. Yamaguchi, J., Yamaguchi, A. D. & Itami, K. C–H bond functionalization: emerging synthetic tools for natural products and pharmaceuticals. *Angew. Chem. Int. Ed.* **51**, 8960–9009 (2012).
18. Vitaku, E., Smith, D. T. & Njardarson, J. T. Analysis of the structural diversity, substitution patterns, and frequency of nitrogen heterocycles among US FDA approved pharmaceuticals. *J. Med. Chem.* **57**, 10257–10274 (2014).
19. Stateman, L. M., Dare, R. M., Paneque, A. N. & Nagib, D. A. Aza-heterocycles via copper-catalyzed, remote C–H desaturation of amines. *Chem* **8**, 210–224 (2022).
20. Hunsdiecker, H. & Hunsdiecker, Cl. Über den Abbau der Salze aliphatischer Säuren durch Brom. *Ber. Dtsch. Chem. Ges.* **75**, 291–297 (1942).
21. Johnson, R. G. & Ingham, R. K. The degradation of carboxylic acid salts by means of halogen—the Hunsdiecker reaction. *Chem. Rev.* **56**, 219–269 (1956).
22. Wilson, C. V. The reaction of halogens with silver salts of carboxylic acids. *Org. React.* https://doi.org/10.1002/0471264180.or009.05 (2011).
23. Duhamel, T. & Muñiz, K. Cooperative iodine and photoredox catalysis for direct oxidative lactonization of carboxylic acids. *Chem. Commun.* **55**, 933–936 (2019).

24. Zeng, Z., Feceu, A., Sivendran, N. & Gooßen, L. J. Decarboxylation-initiated intermolecular carbon–heteroatom bond formation. *Adv. Synth. Catal.* **363**, 2678–2722 (2021).
25. Zhang, H. & Muñiz, K. Selective piperidine synthesis exploiting iodine-catalyzed Csp^3–H amination under visible light. *ACS Catal.* **7**, 4122–4125 (2017).
26. Herold, S., Bafaluy, D. & Muñiz, K. Anodic benzylic C(sp^3)–H amination: unified access to pyrrolidines and piperidines. *Green Chem.* **20**, 3191–3196 (2018).
27. Pandey, G., Laha, R. & Mondal, P. K. Heterocyclization involving benzylic C(sp^3)–H functionalization enabled by visible light photoredox catalysis. *Chem. Commun.* **55**, 9689–9692 (2019).
28. Bafaluy, D. et al. Copper-catalyzed N–F bond activation for uniform intramolecular C–H amination yielding pyrrolidines and piperidines. *Angew. Chem. Int. Ed.* **58**, 8912–8916 (2019).
29. Zhang, Z., Zhang, X. & Nagib, D. A. Chiral piperidines from acyclic amines via enantioselective, radical-mediated δ C–H cyanation. *Chem* **5**, 3127–3134 (2019).
30. Kita, Y. et al. Hypervalent iodine-induced nucleophilic substitution of *para*-substituted phenol ethers. Generation of cation radicals as reactive intermediates. *J. Am. Chem. Soc.* **116**, 3684–3691 (1994).
31. Kita, Y., Takada, T., Mihara, S. & Tohma, H. A novel and direct sulfenylation of phenol ethers using phenyl iodine(III) bis(trifluoroacetate) (PIFA) and various thiophenols. *Synlett* **1995**, 211–212 (1995).
32. Kita, Y., Takada, T., Mihara, S., Whelan, B. A. & Tohma, H. Novel and direct nucleophilic sulfenylation and thiocyanation of phenol ethers using a hypervalent iodine(III) reagent. *J. Org. Chem.* **60**, 7144–7148 (1995).
33. Kita, Y., Takada, T. & Tohma, H. Hypervalent iodine reagents in organic synthesis: nucleophilic substitution of *p*-substituted phenol ethers. *Pure Appl. Chem.* **68**, 627–630 (1996).
34. Kantak, A. A., Potavathri, S., Barham, R. A., Romano, K. M. & Deboef, B. Metal-free intermolecular oxidative C–N bond formation via tandem C–H and N–H bond functionalization. *J. Am. Chem. Soc.* **133**, 19960–19965 (2011).
35. An, X. D. & Xiao, J. Fluorinated alcohols: magic reaction medium and promoters for organic synthesis. *Chem. Rec.* **20**, 142–161 (2020).
36. Roy, S., Panja, S., Sahoo, S. R., Chatterjee, S. & Maiti, D. Enroute sustainability: metal free C–H bond functionalisation. *Chem. Soc. Rev.* **52**, 2391–2479 (2023).
37. Colomer, I., Chamberlain, A. E. R., Haughey, M. B. & Donohoe, T. J. Hexafluoroisopropanol as a highly versatile solvent. *Nat. Rev. Chem.* **1**, 0088 (2017).
38. Motiwala, H. F. et al. HFIP in organic synthesis. *Chem. Rev.* **122**, 12544–12747 (2022).
39. Yu, C., Sanjosé-Orduna, J., Patureau, F. W. & Pérez-Temprano, M. H. Emerging unconventional organic solvents for C–H bond and related functionalization reactions. *Chem. Soc. Rev.* **49**, 1643–1652 (2020).
40. Solyev, P. N. in *Handbook of CH-Functionalization* (ed. Maiti, D.) 1–25 (Wiley, 2022); https://doi.org/10.1002/9783527834242.chf0214
41. Colomer, I., Batchelor-Mcauley, C., Odell, B., Donohoe, T. J. & Compton, R. G. Hydrogen bonding to hexafluoroisopropanol controls the oxidative strength of hypervalent iodine reagents. *J. Am. Chem. Soc.* **138**, 8855–8861 (2016).
42. Eberson, L., Persson, O. & Hartshorn, M. P. Detection and reactions of radical cations generated by photolysis of aromatic compounds with tetranitromethane in 1,1,1,3,3,3-hexafluoro-2-propanol at room temperature. *Angew. Chem. Int. Ed.* **34**, 2268–2269 (1995).
43. Eberson, L., Hartshorn, M. P. & Persson, O. Generation of solutions of highly persistent radical cations by 4-tolylthallium(III) bis(trifluoroacetate) in 1,1,1,3,3,3-hexafluoropropan-2-ol. *J. Chem. Soc., Chem. Commun.* **1995**, 1131–1132 (1995).
44. Kita, Y. & Dohi, T. Pioneering metal-free oxidative coupling strategy of aromatic compounds using hypervalent iodine reagents. *Chem. Rec.* **15**, 886–906 (2015).
45. Wang, X. & Studer, A. Iodine(III) reagents in radical chemistry. *Acc. Chem. Res.* **50**, 1712–1724 (2017).
46. Shchepochkin, A. V., Antipin, F. V., Charushin, V. N. & Chupakhin, O. N. Oxidative C–H functionalization of arenes: main tool of 21st century green chemistry. A review. *Dokl. Chem.* **499**, 123–157 (2021).
47. Ito, M. et al. Enhanced reactivity of [hydroxy(tosyloxy)iodo] benzene in fluoroalcohol media. Efficient direct synthesis of thienyl(aryl)iodonium salts. *Molecules* **15**, 1918–1931 (2010).
48. Huang, J. et al. The lightest organic radical cation for charge storage in redox flow batteries. *Sci. Rep.* **6**, 32102 (2016).
49. Dohi, T. et al. Unusual ipso substitution of diaryliodonium bromides initiated by a single-electron-transfer oxidizing process. *Angew. Chem. Int. Ed.* **49**, 3334–3337 (2010).
50. Nakajima, M. et al. A direct S0→Tn transition in the photoreaction of heavy-atom-containing molecules. *Angew. Chem. Int. Ed.* **59**, 6847–6852 (2020).
51. Narobe, R. & König, B. Transformations based on direct excitation of hypervalent iodine(III) reagents. *Org. Chem. Front.* **10**, 1577–1586 (2023).
52. Mantilla, T., Carrillo, L., Zamudio-Rivera, L. S., Beltrán, H. I. & Farfán, N. Synthesis and characterization of new 2-substituted isoindoline derivatives of α-amino acids. *Org. Prep. Proced. Int.* **33**, 341–349 (2001).
53. Andrade-Jorge, E., Bahena-Herrera, J. R., Garcia-Gamez, J., Padilla-Martínez, I. I. & Trujillo-Ferrara, J. G. Novel synthesis of isoindoline/isoindoline-1,3-dione derivatives under solventless conditions and evaluation with the human D2 receptor. *Med. Chem. Res.* **26**, 2420–2431 (2017).
54. Alvarez-Moreno, M. et al. Managing the computational chemistry big data problem: the ioChem-BD platform. *J. Chem. Inf. Model.* **55**, 95–103 (2015).
55. Nicholas, A. M., de, P. & Arnold, D. R. Thermochemical parameters for organic radicals and radical ions. Part 1. The estimation of the pK_a of radical cations based on thermochemical calculations. *Can. J. Chem.* **60**, 2165–2179 (1982).
56. Albini, A., Mella, M. & Freccero, M. A new method in radical chemistry: generation of radicals by photo-induced electron transfer and fragmentation of the radical cation. *Tetrahedron* **50**, 575–607 (1994).
57. Schmittel, M. & Burghart, A. Understanding reactivity patterns of radical cations. *Angew. Chem. Int. Ed.* **36**, 2550–2589 (1997).
58. Wang, S. et al. Site-selective amination towards tertiary aliphatic allylamines. *Nat. Catal.* **5**, 642–651 (2022).

Acknowledgements

This work was supported by ICIQ, the CERCA Programme/Generalitat de Catalunya, Ministerio de Ciencia e Innovación/Agencia Estatal de Investigación and the Agencia de Gestión de Ayudas Universitarias y de Investigación (AGAUR) (MICINN/AEI/Severo Ochoa Excellence Accreditation 2020-2023–CEX2019-000925-S; grant numbers PID2020-112733GB-I00, PID2020-112825RB-I00 and 2021 SGR 01154). J.X. and J.Z. thank the China Scholarship Council for predoctoral fellowships (CSC202108330066 and CSC201906280437). S.L.-R. thanks the Generalitat de Catalunya for an FI–Agaur predoctoral contract.

Author contributions

J.X. and J.Z. performed the synthetic methodology. J.X., J.Z. and S.K. carried out the experimental mechanistic investigation. J.X. and S.L.-R.

conducted the computational studies. J.X., J.Z., S.K. and E.C. analysed the experimental data. M.H.P.-T. and F.M. contributed to the design of the study and the data analysis. All the authors discussed the results and co-wrote the manuscript.

Competing interests
The authors declare no competing interests.

Additional information
Supplementary information The online version contains supplementary material available at https://doi.org/10.1038/s44160-024-00566-w.

Correspondence and requests for materials should be addressed to Feliu Maseras or Mónica H. Pérez-Temprano.

Peer review information *Nature Synthesis* thanks Yu Lan and the other, anonymous, reviewer(s) for their contribution to the peer review of this work. Primary Handling Editor: Peter Seavill, in collaboration with the *Nature Synthesis* team.